Heliyon 9 (2023) e15915

Contents lists available at ScienceDirect

Heliyon

journal homepage: www.cell.com/heliyon

Research article

Optimizing the fuel economy of hydrostatic power-split system in continuously variable tractor transmission

Guangming Wang [a,*,1], Yehui Zhao [a,b,1], Yue Song [c], Lijun Xue [d], Xiaohan Chen [a]

[a] College of Mechanical and Electronic Engineering, Shandong Agricultural University, Taian, 271018, China
[b] Shandong Provincial Engineering Laboratory of Agricultural Equipment Intelligence, Taian, 271018, China
[c] College of Engineering, Nanjing Agricultural University, Nanjing, 210031, China
[d] College of Information Science and Engineering, Shandong Agricultural University, Taian, 271018, China

ARTICLE INFO

Keywords:
Tractor
Continuously variable transmission
Power split
Energy consumption
Fuel economy

ABSTRACT

The aim of this study is to enhance the fuel economy of a continuously variable tractor transmission by analyzing its energy and fuel consumption. First, we present the principle of a self-developed tractor transmission based on power splitting and examine its parasitic power characteristics. Next, we construct a mathematical model of the hydraulic system, mechanical system, and entire transmission, calibrating the model to ensure the accuracy of subsequent results. We then perform a systematic analysis of the energy and fuel consumption of the tractor transmission. Finally, we optimize the transmission through design and power matching, investigating the impact of changes in parameters and control strategies on the fuel economy of the transmission. The results indicate that fuel consumption can be reduced by 2%–14% through parameter optimization and by an additional 0%–20% through appropriate power matching.

1. Introduction

The tractor is the most important power machinery used in agriculture. Because they consume a significant amount of diesel every year, it is important to design tractors with good fuel economy to ensure the sustainable development of agriculture. The fuel consumption of traditional tractors is largely determined by the performance of the engine [1–4]. Currently available diesel engines have thermal efficiencies exceeding 51%, but they are approaching the limits of their performance.

Hydrostatic power-split continuously variable transmission (CVT) [5,6] can optimize the engine's operation by automatically adjusting the speed of the engine to match the transmission ratio, improving fuel economy. The German manufacturer Fendt was the first to develop the hydrostatic power-split CVT called Vario [7,8], which was installed in its 191 kW Favorit 926 tractor. With 45° variable bent-axis units jointly developed with Sauer Sundstrand (called Sauer Danfoss today), Vario's full-load efficiency with the axle can be maintained at 78%–84%. Soon after, other tractor manufacturers [9–11], such as ZF and Claas, introduced their own CVTs.

Most of these transmissions use multi-range speed regulation [12–14] to eliminate dependence on high-performance hydraulic components and to regulate speed over a wider range while reducing the hydrostatic power portion in each range. For example, the full-load efficiency of HM8 with seven ranges of speed regulation can reach 89%–94%. However, multi-range technology is not always effective in this context. In recent years, some inexperienced manufacturers have begun developing hydrostatic power-split CVTs, but

* Corresponding author.
E-mail address: gavinwang1986@163.com (G. Wang).
[1] These authors contributed equally to this work.

https://doi.org/10.1016/j.heliyon.2023.e15915
Received 1 December 2022; Received in revised form 15 April 2023; Accepted 26 April 2023
Available online 2 May 2023

Nomenclature

n_e, n_t	Output speeds of engine and CVT, respectively. [r/min]
e	Displacement ratio of pump to motor
k	Standing ratio of planetary gear
k_1, k_2	Standing ratios of planetary gears p_1 and p_2, respectively
V_{pmax}, V_m	Rated displacements of pump and motor, respectively. [m^3/rad]
n_p, n_m	Speeds of pump shaft and motor shaft, respectively. [r/min]
C_s	Total leakage coefficient
Δp	Pressure difference between inlet and outlet of the motor. [Pa]
μ	Dynamic viscosity of hydraulic oil. [Pa·s]
T_p, T_m	Torques of pump shaft and motor shaft, respectively. [N·m]
f_p, f_m	Viscosity damping coefficients of pump shaft and motor shaft, respectively. [N·m·s/rad]
n_p, n_m	Speeds of pump shaft and motor shaft, respectively. [r/min]
C_{fp}, C_{fm}	Pressure-dependent friction loss coefficients of pump shaft and motor shaft, respectively
i_{sr}^c	Transmission ratio of conversion mechanism of planetary gear
n_s, n_r, n_c, n_{pl}	Speeds of sun gear, ring gear, carrier, and planet gear, respectively. [r/min]
z_s, z_r, z_{pl}	Numbers of teeth of sun gear, ring gear, and planet gear, respectively
n_{pl}^c	Speed of the planet gear in the conversion mechanism of planetary gear. [r/min]
n_s^c, n_r^c	Speeds of sun gear and ring gear in the conversion mechanism of planetary gear, respectively
T_s, T_r, T_c	Torques of sun gear, ring gear, and carrier, respectively. [N·m]
η_{sr}	Transmission efficiency of planetary gear
m	Modulus of gear
n_{gi}, n_{go}	Input and output speeds of gear pair, respectively
T_{gi}, T_{go}	Input and output torques of gear pair, respectively. [r/min]
η_g	Transmission efficiency of gear pair
i_g	Transmission ratio of gear pair
φ_t	Coefficient of CVT loss
T_e, T_t	Output torques of engine and CVT, respectively. [N·m]
g_e, g_t	Fuel consumption of engine and "engine-transmission" system, respectively. [g/(kw·h)]
i_{R4}^*	Minimum transmission ratio of the CVT range HM_4
Ψ	Common ratio of the CVT
ξ, σ	Objective function and constraint function for CVT energy consumption optimization, respectively

tractors equipped with these transmissions often have insufficient power and high fuel consumption. Without theoretical guidance, the developmental cost of the CVT tractor is unbearable for many manufacturers. The problems related to fuel economy have become a technical bottleneck in the industrialization of CVT tractors in many countries.

To reduce fuel consumption in CVT tractors, there are two approaches: energy-saving design and engine power matching. In the context of energy-saving design, Rossetti and Macor [15] optimized the efficiency of the hydrostatic power-split CVT based on the multi-objective particle swarm optimization (PSO) algorithm, and applied it to different configurations of the planetary gear in subsequent research [16]. Xia et al. [17] reported similar research based on the NSGA-II (non-dominant sorting genetic algorithm II) multi-objective genetic algorithm. In addition to efficiency, researchers have sought to optimize the transmission and torque ratios of the CVT. In the context of engine power matching, Ince and Güler [18] compared the fuel consumption of the hydrostatic power-split CVT and traditional mechanical shift transmission under a specific matching strategy, while Rossetti et al. [19,20] compared the fuel consumption of the hydrostatic power-split CVT and power shift transmission. Their results clearly showed that the fuel economy of the hydrostatic power-split CVT is significantly better than that of traditional transmissions.

However, past studies have not uncovered the laws of influence and underlying mechanisms that affect energy and fuel consumption in transmissions, making it challenging to obtain generally correct and systematic information. Additionally, previous research on CVT fuel economy has not focused extensively on tractors, and the control strategies and performance evaluation criteria [21–23] used in traditional road vehicles are not easily transferable to tractors operating in complex conditions. To overcome the limitations of prior research and provide sound theoretical support for the development of CVT tractors, this study uses a newly developed CVT as a case example to systematically examine the design of the transmission and the theory of power matching in hydrostatic power-split tractor transmissions.

2. Methods and materials

2.1. Powertrain

Fig. 1 shows the powertrain of the hydrostatic power-split CVT, which is a typical planetary input-coupled CVT with a hydrostatic starting range HY and four hydrostatic power-splitting ranges, HM_1-HM_4, enabling variable tractor speed regulation between 0 and 50 km/h. A Simpson planetary gear set consisting of two standard planetary gears, p_1 and p_2, works alternately in the HM_1/HM_3 and HM_2/HM_4 ranges, respectively. The CVT speed in each range can be adjusted by varying the displacement of the variable-displacement pump, while wet clutches enable shifting between adjacent ranges.

If the motor and pump shafts rotate in the same direction, the pump displacement is positive; otherwise, it is negative. To simplify later derivations, we define the "low-speed side" of the range as the range where the pump displacement is positive in HM_1 and HM_3 or negative in HM_2 and HM_4, while the "high-speed side" is defined as the remaining range. Hydraulic transmissions consume more energy than mechanical transmissions, and the energy consumption of the CVT increases with the portion of hydrostatic power. Fig. 2 shows the portion of hydrostatic power for each range of the power-split CVT. The maximum hydrostatic power portion on the low-speed side of each range was 0.44, while the maximum on the high-speed side was 0.23. This phenomenon was due to parasitic power consumption inside the hydraulic system on the low-speed side of each range, which increased the energy consumption of the transmission without being output.

2.2. Modeling

2.2.1. Swash-plate axial piston units

The swash-plate axial piston units consist of a variable-displacement pump and a fixed-displacement motor with the same rated displacement. Hydraulic oil is typically treated as an incompressible fluid. As a result, the pump flow equals the sum of the motor flow and leakage, given by:

$$\pi V_{pmax} n_p e \,/\, 30 = \pi V_m n_m \,/\, 30 + C_s \Delta p \left(V_{pmax} + V_m\right) / \mu \tag{1}$$

where V_{pmax} and V_m are the rated displacements of the pump and motor, respectively, m^3/rad; n_p and n_m are the speeds of the pump shaft and motor shaft, respectively, r/min; e is the displacement ratio of the pump to motor; C_s is the total leakage coefficient; Δp is the pressure difference between the inlet and outlet of the motor, Pa; μ is the dynamic viscosity of the hydraulic oil, Pa·s.

According to the law of energy conservation, the pressure-induced energy of the hydraulic motor should be equal to its converted mechanical energy. Thus, we get:

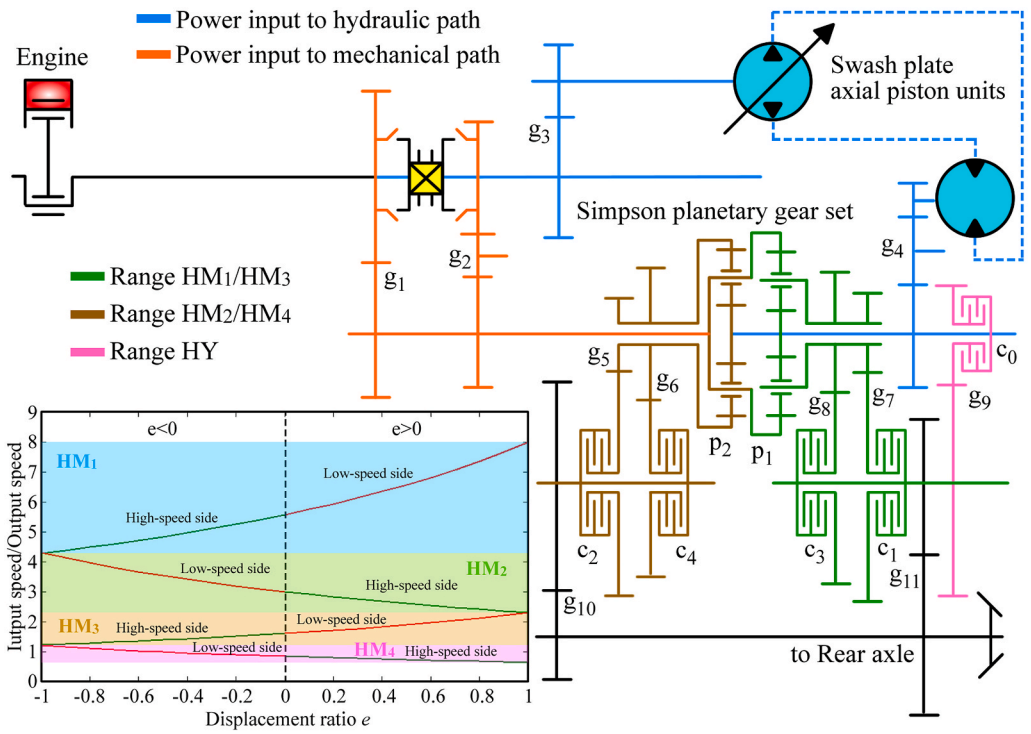

Fig. 1. Powertrain of hydrostatic power-split transmission.

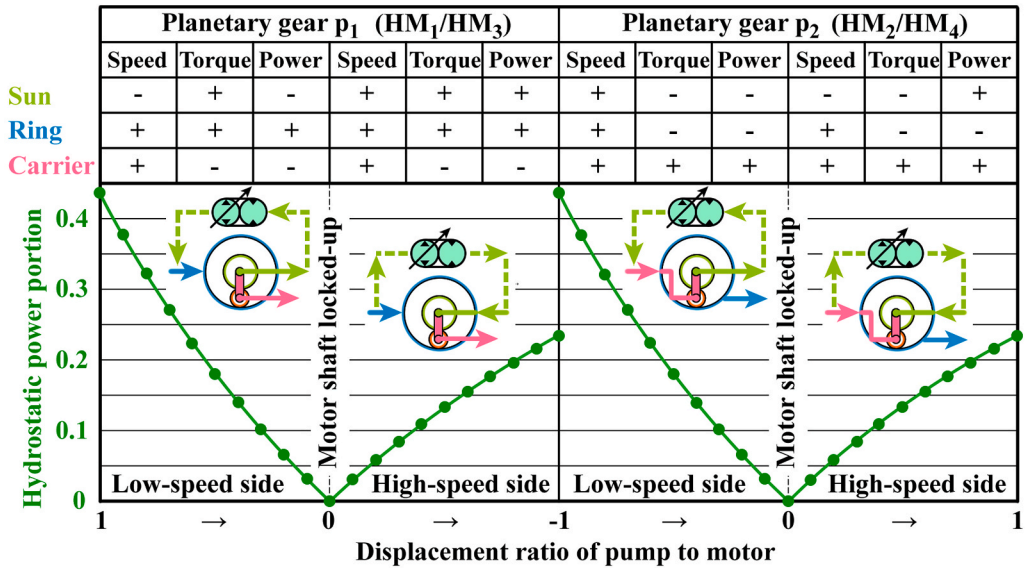

Fig. 2. Analysis of the transmission parasitic power.

$$\Delta pV_m = T_m + f_m n_m \pi/30 + C_{fm}\Delta pV_m \tag{2}$$

where T_m is the torque of the motor shaft, N·m; f_m is the viscosity damping coefficient of the motor shaft, N·m·s/rad; C_{fm} is the pressure-dependent friction loss coefficient of the motor shaft.

Similarly, the torque of the pump can be deduced as follows:

$$-\Delta pV_{pmax}e = -T_p + f_p n_p \pi/30 - C_{fp}\Delta pV_{pmax}e \tag{3}$$

where T_p is the torque of the pump shaft, N·m; f_p is the viscosity damping coefficient of the pump shaft, N·m·s/rad; C_{fp} is the pressure-dependent friction loss coefficient of the pump shaft.

2.2.2. *Planetary gears and gear pairs*

The rotational speeds of the sun gear, ring gear, and carrier of the standard planetary gear satisfy the following relationship:

$$i_{sr}^c = (n_s - n_c)/(n_r - n_c) = -z_r/z_s = -k \tag{4}$$

where i_{sr}^c is the transmission ratio of the planetary gear conversion mechanism; n_s, n_r, and n_c are the speeds of the sun gear, ring gear, and carrier, respectively, r/min; z_s and z_r are the numbers of teeth of the sun gear and ring gear, respectively; k is the standing ratio of the planetary gear. Therefore, we get:

$$n_s + kn_r - (1+k)n_c = 0 \tag{5}$$

when the power flows from the sun gear to the ring gear in the conversion mechanism, we get:

$$T_r n_r^c + T_s\left(n_s^c\right)\eta_{sr} = 0 \tag{6}$$

$$T_r + T_s(n_s - n_c)/(n_r - n_c)\eta_{sr} = T_r - T_s k\eta_{sr} = 0 \tag{7}$$

where T_s and T_r are the torques of the sun gear and ring gear, respectively, N·m; n_s^c and n_r^c are the speeds of the sun gear and ring gear in the conversion mechanism of the planetary gear, respectively, r/min; η_{sr} is the transmission efficiency of the planetary gear. Thus, we obtain:

$$T_s = T_r/(k\eta_{sr}) \tag{8}$$

Considering that the torque among the three basic components meets the relationship

$$T_r + T_s + T_c = 0 \tag{9}$$

where T_c is the torque of the carrier, N·m.

Eq. (8) can also be expressed as

$$T_s = -T_c / (1 + k\eta_{sr}) \tag{10}$$

Similarly, when the power flows from the ring gear to the sun gear, the following equation can be obtained:

$$T_s = T_r / (k / \eta_{sr}) \tag{11}$$

$$T_s = -T_c / (1 + k / \eta_{sr}) \tag{12}$$

The power flow direction in the planetary gear conversion mechanism can be determined through force analysis, as shown in Fig. 3 (a)–(b). To ensure force balance of the planet gears, when power flows from the sun gear to the ring gear, the torque direction of the carrier should be opposite to that of the ring gear and the sun gear. Therefore, the conditions for identifying power flow from the sun gear to the ring gear are as follows: planetary gear p_1 must satisfy $n_{pl}^c \times T_c > 0$, and planetary gear p_2 must satisfy $n_{pl}^c \times T_r < 0$. Similarly, when power flows from the ring gear to the sun gear, planetary gear p_1 must satisfy $n_{pl}^c \times T_c < 0$, and planetary gear p_2 must satisfy $n_{pl}^c \times T_r > 0$.

The rotational speed of the planet gear in its conversion mechanism can be obtained by the following method:

Because the linear velocities of the ring gear and planet gear at the pitch point are equal, we have:

$$m(z_s + z_{pl})n_c + mz_{pl}n_{pl} = mz_r n_r \tag{13}$$

where m is the modulus of the gear; z_{pl} is the number of teeth of the planet gear.

Note that

$$z_r = z_s + 2z_{pl} \tag{14}$$

Substituting Eqs. (4), (5) and (14) into Eq. (13) yields:

$$n_{pl} = (kn_r - n_s) / (k - 1) \tag{15}$$

where n_{pl} is the speed of the planet gear, r/min.

Thus, the rotational speed of the planet gear in its conversion mechanism is

$$n_{pl}^c = n_{pl} - n_c = (kn_r - n_s) \Big/ (k - 1) - n_c \tag{16}$$

where n_{pl}^c is the speed of the planet gear in the conversion mechanism of the planetary gear, r/min.

Equations for the speed and torque of each gear can be obtained as follows based on analyses similar to the above:

$$n_{go} = n_{gi} / i_g \tag{17}$$

$$T_{gi} = T_{go} / \left(i_g \eta_g \, exp\left(sign\left(n_{gi} T_{go}\right)\right)\right) \text{ or } T_{gi} = T_{go} / \left(i_g \eta_g \, exp\left(sign\left(-n_{go} T_{gi}\right)\right)\right) \tag{18}$$

where T_{gi} and T_{go} are the input and output torques of the gear pair, respectively, r/min; i_g is the transmission ratio of the gear pair; η_g is

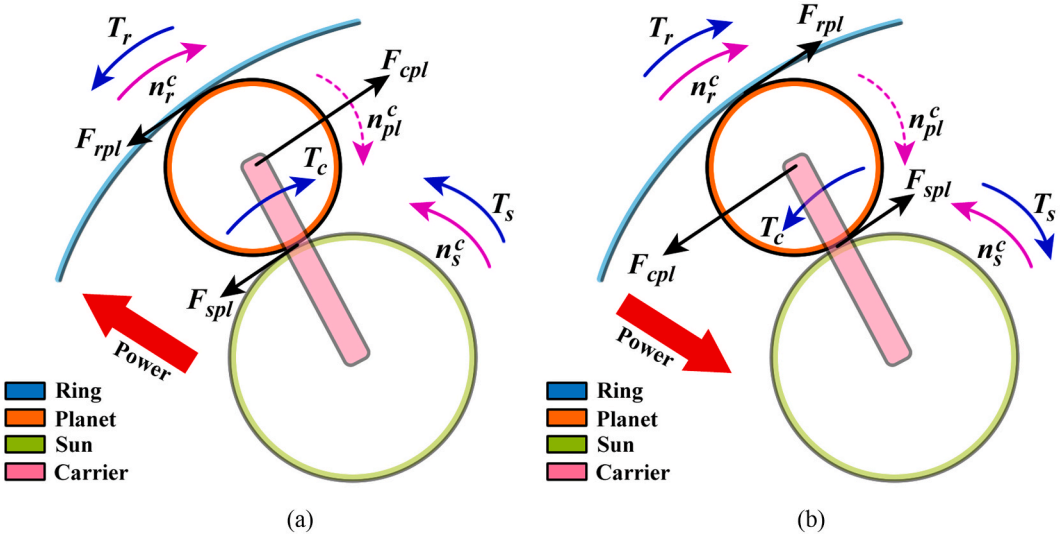

Fig. 3. Force analysis of the mechanism of planetary gear conversion under different directions of power flow: (a) Power flows from the sun gear to the ring gear. (b) Power flows from the ring gear to the sun gear.

the transmission efficiency of the gear pair; n_{gi} and n_{go} are the input and output speeds of the gear pair, respectively, r/min.

2.2.3. Power-split transmission

For a given input speed, displacement of the pump, and load torque, the speed and torque of each shaft of the CVT can be solved for by Eqs. 1–18, as shown in Fig. 4. The coefficient of loss Φ_t can then be used to determine the energy consumption of the CVT according to the ratio of output power to input power, as shown in Eq. (19):

$$\varphi_t = 1 - (n_t T_t) / (n_e T_e) \tag{19}$$

where Φ_t is the coefficient of CVT loss; n_e and n_t are the output speeds of the engine and CVT, respectively, r/min; T_e and T_t are the output torques of the engine and CVT, respectively, N·m.

In the given equations, most mechanical parameters, such as gear transmission ratios, are known. The transmission efficiency of each gear pair can be obtained by consulting relevant design manuals according to actual machining accuracy and operating environment. However, f_p, f_m, and C_s/μ are important parameters that have a significant impact on CVT energy consumption and are difficult to determine. These parameters can be calibrated by limited tests under different working conditions, using the following calibration process:

Step 1. Measure the pressure difference between the inlet and outlet of the pump under different CVT ranges and pump displacement. Adjust f_m at intervals to make the simulation results of pressure difference consistent with test results.

Step 2. Measure the output speed and input torque of the CVT under different loads and pump displacement. Adjust C_s/μ at intervals to make the simulation results of CVT output speed consistent with test results.

Step 3. Adjust f_p at intervals to make the simulation results of CVT input torque consistent with test results.

Calibration can be carried out in any CVT range. In this study, the calibration of pressure difference was carried out in ranges HM_1 and HM_2, and a magnetic powder brake suitable for low-speed loading was used as the loader. The calibration of speed and torque was carried out in range HM_4, and a dynamometer suitable for high-speed loading was used as the loader. To avoid dynamic load interference in the calibration process, the engine was operated in idle mode during the test. The test bench used for model calibration is shown in Fig. 5 (a). The calibration curve and data are shown in Fig. 5 (b)–(c), Table 1, and Table 2. The average calibration errors of pressure difference, speed, and torque are −0.0808 MPa, 0.2569 r·min^{-1}, and −0.6109 N m, respectively, which are sufficient for the research needs of this study.

3. Results

3.1. Energy consumption

According to research by Renius and Resch [9,25], a tractor typically operates at a speed of 4–20 km/h throughout its lifecycle. Thus, we examined the energy consumption of a CVT tractor operating within this speed range, as it is mainly used for farmland operation. Using the aforementioned model, we obtained the coefficient of CVT loss at any speed and torque of the engine, as depicted in Fig. 6 (a)–(i). The results of our calculations are as follows:

(1) The higher the output power of the CVT, the lower its energy consumption for the same speeds of the tractor and engine. This is due to a lower increase in the loss of CVT power compared to the increase in the total power, resulting in a reduced ratio of loss of the CVT power to the total power.
(2) The contour line of energy consumption of the CVT for the same speed and range of the tractor is "U" shaped. This is because the higher the absolute value of the displacement of the pump, the higher the portion of hydrostatic power and the energy consumption of the CVT. As the engine speed increases, the displacement of the pump first decreases to zero and then increases in

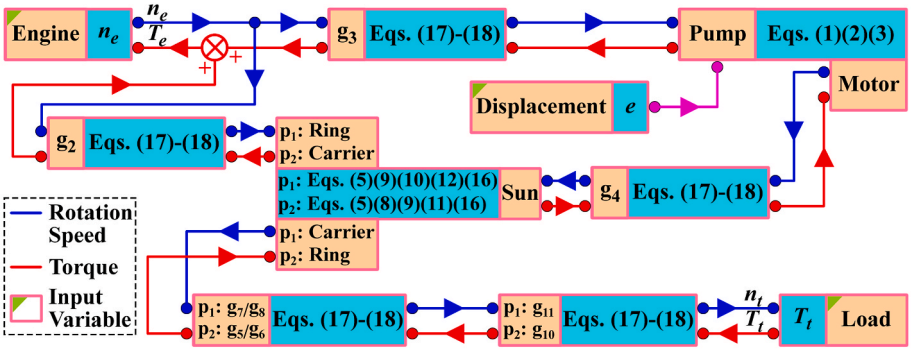

Fig. 4. Flowchart of calculation of the rotational speed and torque of each transmission shaft.

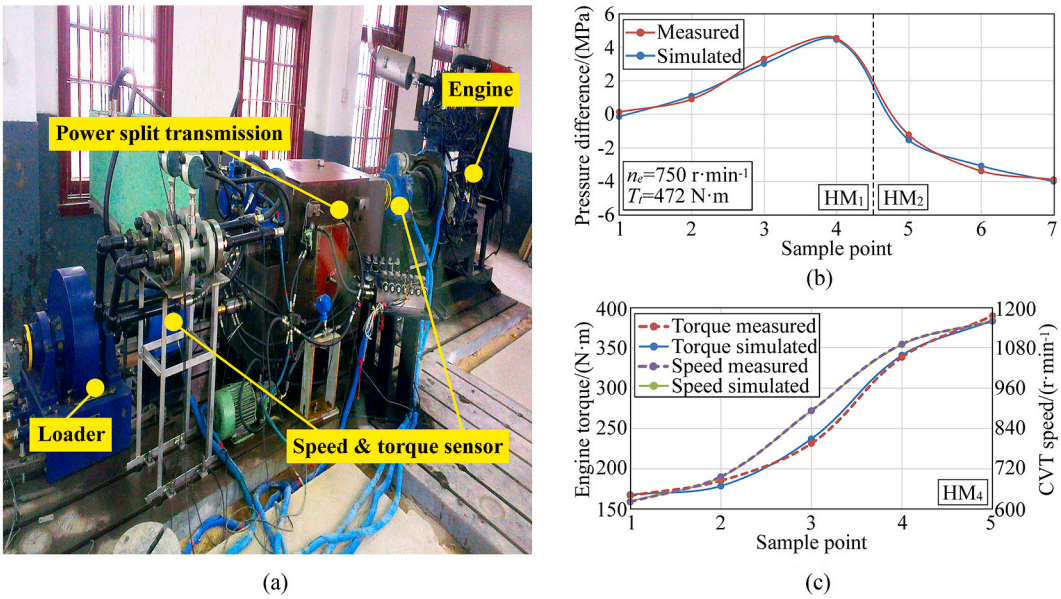

Fig. 5. Test calibration of CVT model for energy consumption calculation. (a) Test bench (reproduced from Ref. [24]). (b) Calibration results of pressure difference. (c) Calibration results of engine torque and CVT speed.

Table 1
Calibration results of pressure difference between inlet and outlet of the pump.

Sample point	Range	e	Measured/(MPa)	Simulated/(MPa)	Absolute error/(MPa)
1	HM$_1$	1	0.1308	−0.1460	−0.2768
2	HM$_1$	0.42	0.8958	1.0923	0.1965
3	HM$_1$	−0.4	3.3095	3.0257	−0.2838
4	HM$_1$	−1	4.5493	4.4674	−0.0819
5	HM$_2$	−1	−1.2289	−1.5427	−0.3138
6	HM$_2$	−0.43	−3.3975	−3.0881	0.3094
7	HM$_2$	0	−3.9035	−4.0188	−0.1153

Table 2
Calibration results of CVT output speed and input torque.

Sample point	e	n_e/(r·min^{-1})	T_t/(N•m)	n_t/(r·min^{-1})			T_e/(N•m)		
				Measured	Simulated	Absolute error	Measured	Simulated	Absolute error
1	−1	748.9642	129.209	621.1877	622.7351	1.5474	166.5373	167.7689	1.2316
2	−0.73	748.6838	138.8624	696.1852	694.8465	−1.3387	184.9833	178.4467	−6.5366
3	0	749.3272	164.5161	892.1236	892.0024	−0.1212	231.1762	236.9146	5.7384
4	0.73	749.6422	187.7536	1089.8956	1088.647	−1.2486	337.9093	340.3149	2.4056
5	1	748.8887	192.7692	1157.8764	1160.322	2.4456	389.3009	383.4074	−5.8935

the opposite direction to maintain the tractor's speed at the specified value. This causes the energy consumption of the CVT to first decrease and then increase with an increase in engine speed.

(3) The energy consumption of the CVT on the high-range side of the shift point is significantly higher than on the low-range side, for the same tractor speed and output power of the CVT. This is because the high-range side of the shift point is also the low-speed side of the range where parasitic power is generated, which increases the energy consumption of the CVT.

(4) A combination of low engine speed and high range reduces the energy consumption of the CVT for the same tractor speed and output power of the CVT. This is due to a decrease in the input speed of the CVT, which reduces the energy consumption caused by the viscous damping of the transmission system. When a high range is used, the torque of the engine increases due to a reduction in the transmission ratio, further reducing the energy consumption of the CVT.

3.2. *Fuel economy*

In this study, the *system fuel consumption* of the "engine-transmission" system, denoted as g_t, is used as an evaluation index of the

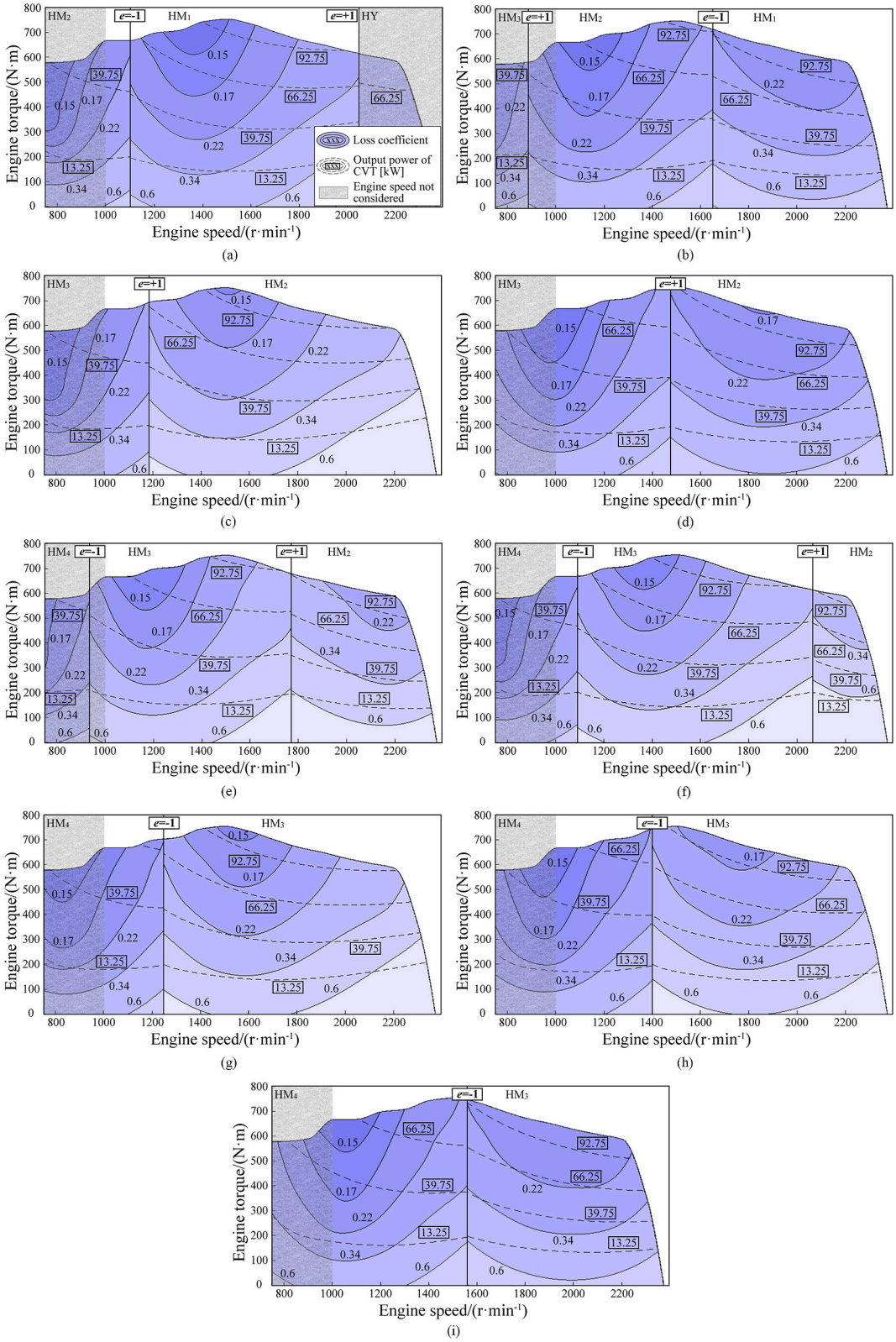

Fig. 6. Map of energy consumption of the CVT at different tractor speeds: (a) 4 km/h (b) 6 km/h (c) 8 km/h (d) 10 km/h (e) 12 km/h (f) 14 km/h (g) 16 km/h (h) 18 km/h (i) 20 km/h.

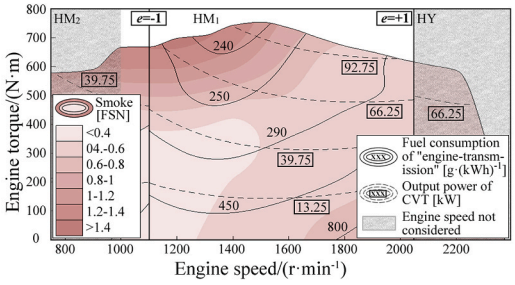

(a)

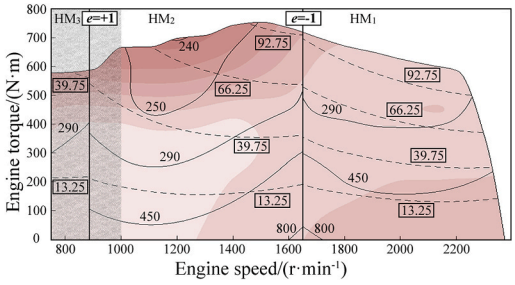

(b)

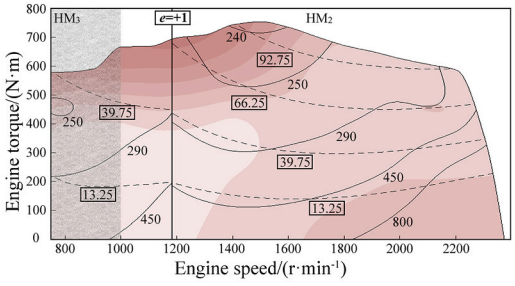

(c)

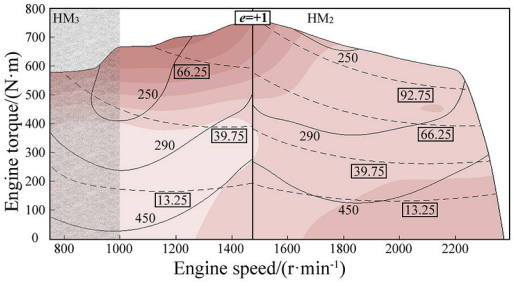

(d)

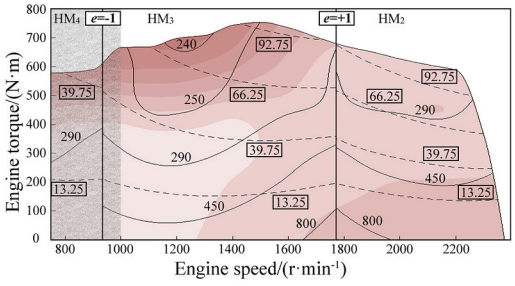

(e)

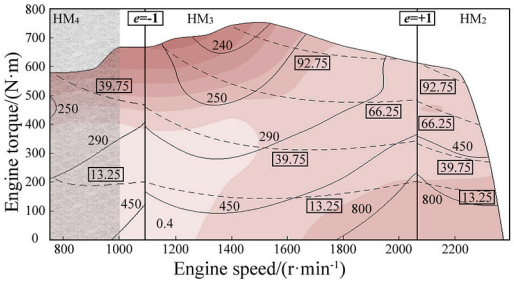

(f)

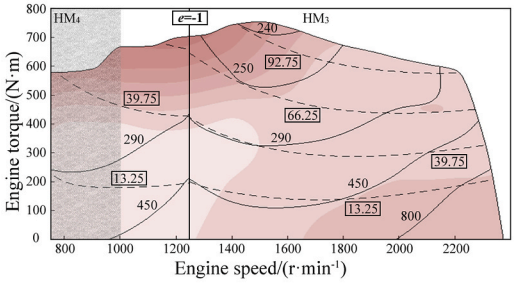

(g)

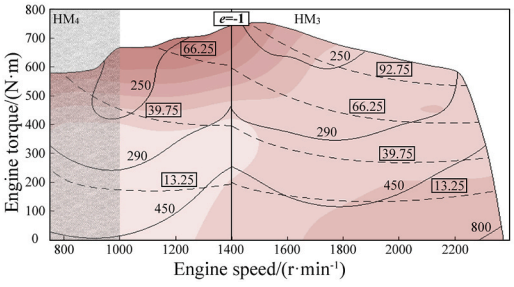

(h)

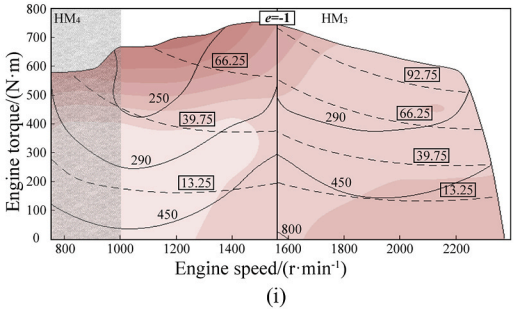

(i)

(caption on next page)

Fig. 7. Map of system fuel consumption at different tractor speeds: (a) 4 km/h (b) 6 km/h (c) 8 km/h (d) 10 km/h (e) 12 km/h (f) 14 km/h (g) 16 km/h (h) 18 km/h (i) 20 km/h.

tractor's fuel economy, and can be expressed as follows [26,27]:

$$g_t = g_e / (1 - \varphi_t) \tag{20}$$

where g_e and g_t are the fuel consumption of the engine and "engine-transmission" system, respectively, in g/(kw·h).

System fuel consumption physically represents the fuel consumed by the engine per unit output work of the CVT. The map of energy consumption of the CVT can be converted into the map of system fuel consumption through Eq. (20), based on data on the loss coefficient in the energy consumption of the map of the CVT above and the data on fuel consumption in the map of the engine, as shown in Fig. 7 (a)–(i). The distribution of smoke in the engine is marked in the map to analyze the characteristics of emissions of the CVT tractor. The results of the calculation showed the following:

(1) For the same speed and range of the tractor, the contour line of system fuel consumption was also "U" shaped due to the significant influence of energy consumption of the CVT on the fuel economy of the tractor.

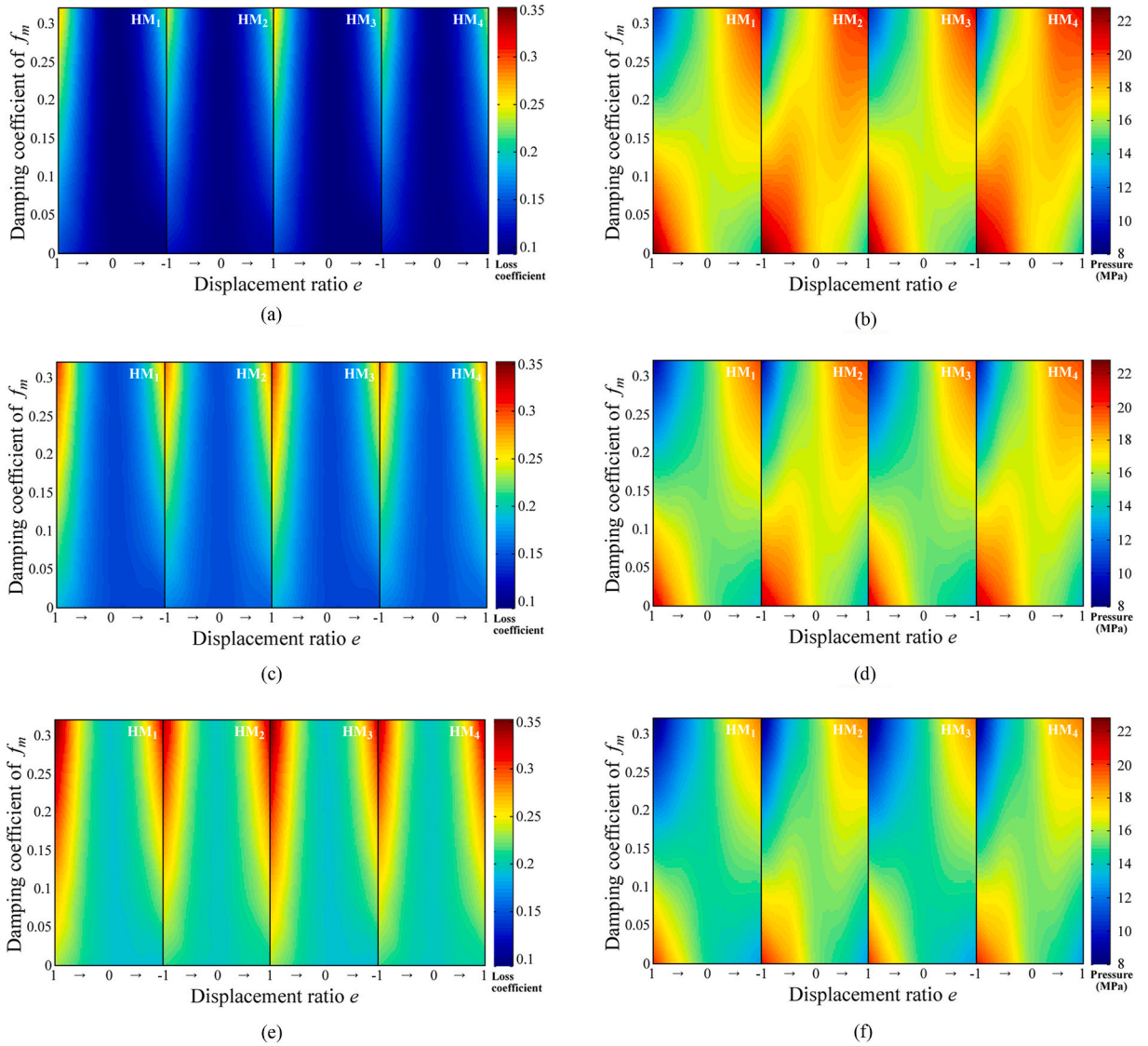

Fig. 8. Influence of hydraulic parameters on the energy consumption of the CVT: (a) Influence of f_m on the CVT loss when $f_p = 0$. (b) Influence of f_m on the pump pressure when $f_p = 0$. (c) Influence of f_m on the CVT loss when $f_p = 0.12$. (d) Influence of f_m on the pump pressure when $f_p = 0.12$. (e) Influence of f_m on the CVT loss when $f_p = 0.24$. (f) Influence of f_m on the pump pressure when $f_p = 0.24$.

(2) Some laws from energy consumption analysis are still applicable to the analysis of the fuel economy of the tractor, owing to the significant influence of energy consumption by the CVT on system fuel consumption. For example, a combination of low engine speed and a high CVT range is still an effective approach to ensure the fuel economy of the tractor.
(3) The distribution of system fuel consumption changed with tractor speed, but the map of distribution of smoke in the engine was fixed and made it difficult to ensure the fuel economy of the tractor while reducing its emissions when controlling the engine and the CVT.

4. Discussion

4.1. Design-based optimization

According to Eqs. (1)–(3), five parameters of the hydraulic system, f_p, f_m, C_s/μ, 1-C_{fp}, and 1-C_{fm}, may affect the energy consumption of the CVT. However, among them, only f_m and f_p are controllable in the design of the CVT and can affect its energy consumption. Fig. 8 (a)–(f) shows their influence, with the data calculated based on the same external characteristic point of the engine, i.e., $n_e = 1500$ r/min and $T_e = 752$ N m. Results showed that:

(1) For the same ranges and values of f_p and f_m, the greater the absolute displacement of the pump, the higher the energy consumption of the CVT. Energy consumption on the low-speed side of the range was higher than that on the high-speed side due to the difference in energy consumed by the CVT caused by hydrostatic power and parasitic power.
(2) For the same range and value of f_p, when f_m was large, the difference in pressure between the inlet and outlet of the pump on the low-speed side of the range was lower than that on the high-speed side, and the reverse case occurred when f_m was small. Reducing f_m led to a decrease in energy consumption of the motor on the low-speed side, offsetting part of the CVT's energy loss caused by parasitic power. On the high-speed side, the energy consumption of the CVT showed a trend of decrease due to a decrease in friction loss caused by f_m. A smaller f_m reduced the difference in energy consumption between the low-speed side and the high-speed side of the range, thus reducing the overall energy consumption of the CVT.
(3) For the same range and value of f_m, the energy consumption of the CVT increased with the value of f_p, which was proportional to the friction-induced torque generated at the same input speed. The actual f_p might have been small, but the viscous damping related to the input speed in the entire transmission system was superimposed on the pump shaft and could not be ignored.

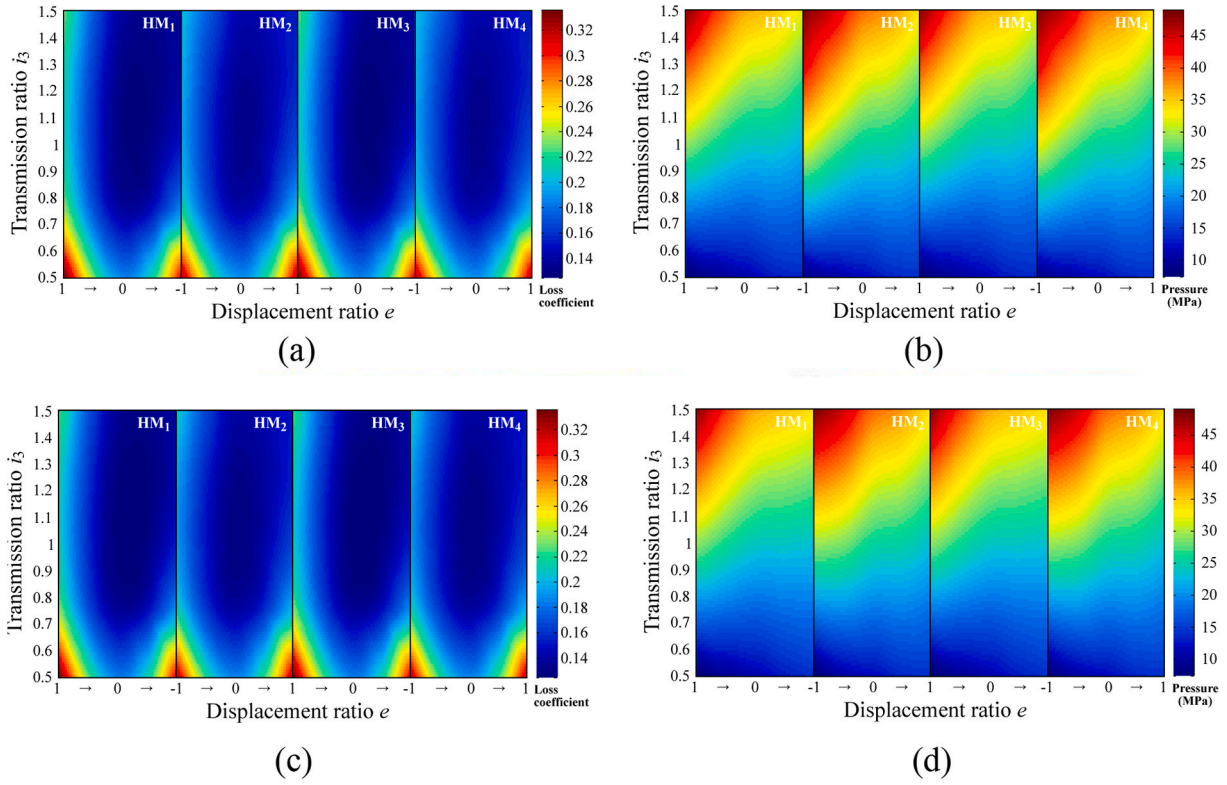

Fig. 9. Influence of mechanical parameters on energy consumption of the CVT: (a) Influence of i_3 on the CVT loss when $k_2 = 1.8$. (b) Influence of i_3 on the pump pressure when $k_2 = 1.8$. (c) Influence of i_3 on the CVT loss when $k_2 = 3$. (d) Influence of i_3 on the pump pressure when $k_2 = 3$.

The parameters of the mechanical system mainly refer to the parameters of gears of the transmission. We focus on the effect of the gear pair g_3 transmission ratio and planetary gears p_1 and p_2 standing ratios on the CVT energy consumption, as illustrated in Fig. 9 (a)–(d). It is worth noting that the transmission is an equal-ratio CVT that adheres to the following equation:

$$k_1 = k_2 + 1 \tag{21}$$

The calculations yielded the following results:

(1) With the same planetary gear standing ratio, increasing the transmission ratio i_3 led to a significant rise in pressure difference between the pump's inlet and outlet while lowering the pump and motor rotational speeds. As mentioned earlier, both decreasing the pump input speed and increasing the pressure difference between the pump inlet and outlet can reduce energy consumption. However, the pump and motor had maximum pressure limits, limiting the transmission ratio i_3. Thus, it was necessary to verify the pump and motor working pressures when determining i_3.
(2) With the same transmission ratio i_3, the planetary gear standing ratio had little impact on the energy consumption of the CVT.

The above analysis indicates that reducing f_p and f_m and increasing the transmission ratio i_3 are effective ways to reduce the energy consumption of the CVT. f_p determines the energy loss associated with the input speed of the CVT, and its value is affected by the viscous damping of the entire transmission, not just the pump. Therefore, optimizing the bearings and gears can help reduce the value of f_p. Similarly, f_m can also be optimized, but a more convenient method is to use a fixed bent-axis motor instead of a swash-plate motor, as it usually has lower frictional loss [28].

In the design of the CVT, it is easier to reduce energy consumption by optimizing the gear parameters than by optimizing the parameters of the hydraulic system. However, the coupling relationship between the parameters must be considered. Generally, the optimization problem needs to determine the optimization variables, the objective function, and the constraint conditions.

(1) Optimization variables. To maintain the speed regulating range of the tractor before and after optimization, the gear parameters of the CVT need to be determined by Eq. (21) and Eqs. 22–26:

$$i_2 = i_3 i_4 (k_2 + 1)(\Psi - 1) / (\Psi + 1) \tag{22}$$

$$\tau_1 = i_6 i_{10} = 2 \times i_{R4}^* \Psi / [(\Psi - 1) k_2 i_3 i_4] \tag{23}$$

$$\tau_2 = i_8 i_{11} = \tau_1 \Psi k_2 / (k_2 + 2) \tag{24}$$

$$\tau_3 = i_5 i_{10} = \tau_2 \Psi (k_2 + 2) / k_2 \tag{25}$$

$$\tau_4 = i_7 i_{11} = \tau_3 \Psi k_2 / (k_2 + 2) \tag{26}$$

where i_{R4}^* is the minimum transmission ratio of the CVT range HM_4, which determines the maximum driving speed of the tractor; Ψ is the is the common ratio of this equal-ratio CVT. Note that the transmission ratio of gear pairs g_5, g_6, g_7, g_8, g_{10}, and g_{11} is not significant, as the theoretical energy consumption of the CVT depends only on their product τ_x (where $x = 1, 2, 3, 4$). Once the parameters i_3, i_4, and k_2 are specified, all the CVT parameters k_1, i_2, and τ_x used for energy consumption calculation can be uniquely determined.

(2) Objective function: Due to the high input speed and low input torque, the CVT has the highest full-load energy consumption at the rated operating point of the engine (2200 r·min^{-1}, 584 N m). We evaluate the energy consumption level of the CVT using the average value of the CVT loss coefficients under six working conditions at the engine's rated speed and torque: ① Range HM_1, $e = -1$; ② Range HM_1, $e = 0$; ③ Range HM_1, $e = 1$; ④ Range HM_2, $e = -1$; ⑤ Range HM_2, $e = 0$; ⑥ Range HM_2, $e = 1$. Note that due to the same transmission structure, the CVT theoretically has the same full-load energy consumption in ranges HM_1 and HM_3, as well as in ranges HM_2 and HM_4.
(3) Constraint conditions: The CVT has a maximum input torque of 752 N m when the engine operates at 1500 r/min. To avoid excessive pressure in the hydraulic system, the pressure difference between the inlet and outlet of the pump should not exceed 30 MPa under this working condition.

To summarize, the energy consumption optimization of the CVT can be described by Eq. (27):

$$\begin{cases} min & \xi(X, \mathrm{HM}_i, e) = \sum_{i,e} \varphi_t / 6 & n_e = 2200 \text{ r} \bullet \text{min}^{-1}, T_e = 584 \text{ N} \bullet \text{m} \\ & & \forall i = 1, 2, e = 0, \pm 1 \\ s.t. & \max(\sigma(X, \mathrm{HM}_i, e) = |\Delta p|) \le 30 \text{ MPa} & n_e = 1500 \text{ r} \bullet \text{min}^{-1}, T_e = 752 \text{ N} \bullet \text{m} \\ & & \forall i = 1, 2, e = 0, \pm 1 \\ & X = (i_3, i_4, k_2), & i_3 \in [0.5, 1.5], i_4 \in [1, 3], \\ & & k_2 \in \{1.8, 2.15, 2.55, 3\} \end{cases} \tag{27}$$

where ξ is the objective function, and σ is the constraint function.

There are only three free variables in this problem, of which the value of k_2 is standardized, and it can only be taken from the relevant design manuals to meet the tooth matching requirements. Therefore, the solution domain of this optimization problem can be visualized. The domain analysis facilitates searching for the optimal solution, and it is simpler than traditional methods like genetic algorithms, and helps identify the impact of parameter matching on transmission energy consumption. Fig. 10 (a)–(b) shows the operation process and results of domain analysis. The calculations showed that (1) the energy consumption of CVT decreases significantly with an increase in i_3, which agrees with the conclusion shown in Fig. 9, but i_4 and k_2 do not impact energy consumption; (2) k_2 affects the working pressure of the pump to some extent, but values of 1.8 and 3 are not considered due to design difficulties in the planetary gears' manufacturing, assembly, material selection, and structural size. Therefore, the standing ratio of p_2 can only be 2.15 or 2.55. Before optimization, k_2 is 2.55, and i_3 is the only parameter optimized, with i_3 values searched from 0.5 to 1.5 at an interval of 0.1, resulting in an optimal solution of $i_3 = 1$ that meets the constraint conditions.

Fig. 11 (a)–(b) shows the calculated energy consumption of the CVT map before and after optimization under a tractor speed of 8 km/h, when adjusting the transmission ratio of gear pair g_3 from its current value of 0.678–1 while keeping the range of speed regulation of the CVT constant. The results of the calculation indicate a significant decrease in energy consumption of the CVT after optimization.

4.2. Matching-based optimization

We traversed each interpolation point on the contours of the CVT output power in the system fuel consumption map for each tractor speed, obtaining the point of the lowest fuel consumption under specified conditions. If the output power contour crossed multiple ranges, we determined the optimum range and corresponding engine speed through a fuel consumption comparison. Only the contour of the output power with a smoke value less than one was considered when searching for the lowest system fuel consumption. The optimal engine speed, system fuel consumption, and smoke distribution maps were obtained by repeating the search under different speeds and output powers. Fig. 12 (a)–(h) shows the power matching results of the "engine-transmission" system before and after optimizing the transmission ratio i_3. Results show that:

(1) The fuel economy of the 132.5 kW CVT tractor is worst when operating under light loads. Effective control of the transmission system is necessary when the load power is less than 40 kW.

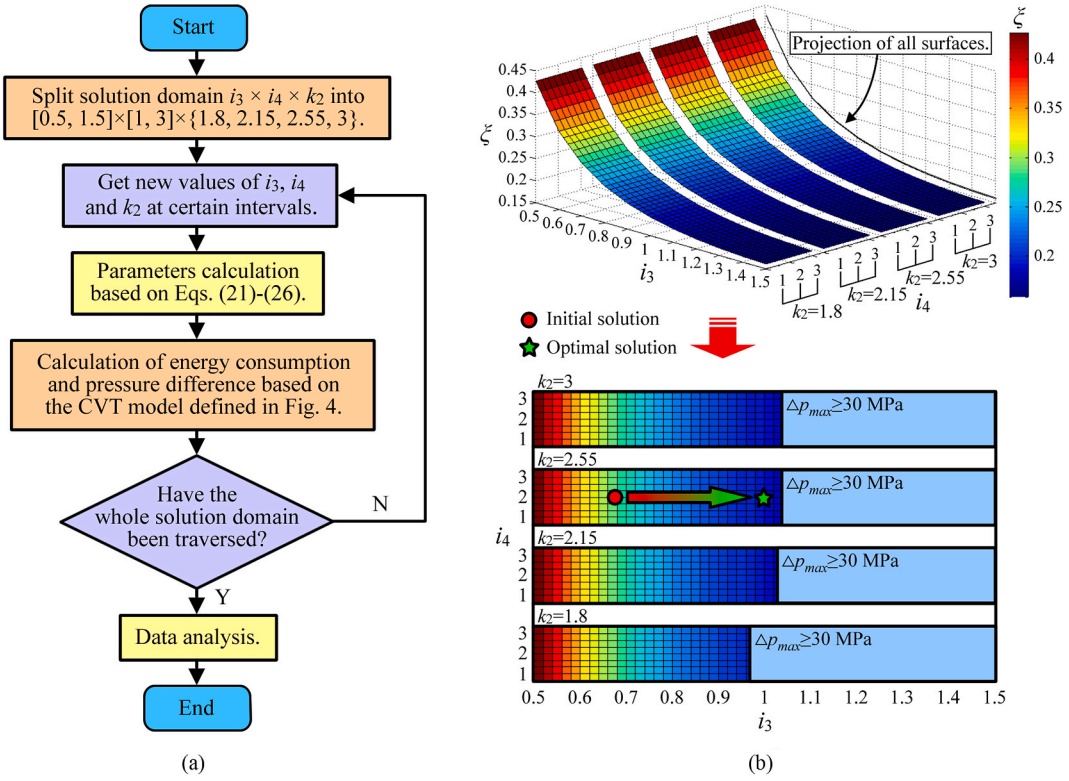

Fig. 10. Optimization of CVT parameters based on solution domain analysis: (a) Operation process of solution domain analysis. (b) Results of solution domain analysis.

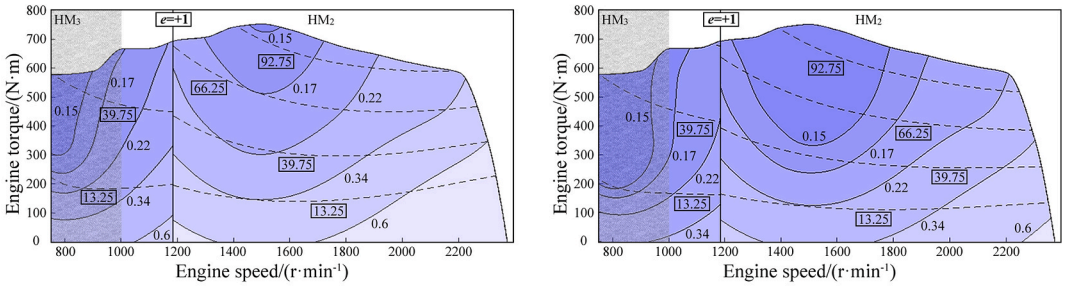

Fig. 11. Influence of the transmission ratio of gear pair g_3 on the energy consumption of the CVT at $V_t = 8$ km/h: (a) $i_3 = 0.678$; (b) $i_3 = 1$.

(2) To save fuel and reduce emissions, reducing the engine speed when operating with a light load is important. However, increasing the engine speed is necessary to meet the required output power as the load increases. The optimal engine speed depends only on the load power, not the tractor's speed, which is significant for developing a simple control strategy.
(3) Optimizing the transmission ratio i_3 not only reduces the energy consumption of the CVT but also has a significant impact on the fuel economy and emissions of the engine-transmission system. Changing the transmission ratio from 0.678 to 1 reduces the system fuel consumption of the tractor by 2%–14% under all working conditions, and the engine's smoke emissions decreased. Although the level of smoke increased under some heavy load operations, it was still less than the one set by the matching rules in this study.

We compared the influence of different control strategies on the fuel economy of a tractor by using an optimized CVT and focusing on optimizing the transmission ratio i_3. Since energy consumption greatly affects fuel economy, we aimed to have the tractor CVT work near the mechanical point to reduce energy consumption caused by hydrostatic split power. This strategy, referred to as "zero-displacement control" (ZD control), makes the displacement of the variable-displacement pump nearly zero, resulting in a CVT equivalent to an ordinary mechanical transmission with four gears. In contrast, "full-displacement control" (FD-I control) shown in Fig. 12 limits emissions by the engine, specifically requiring smoke<1. To systematically evaluate the performance of FD control, we also analyzed "full-displacement control" without considering emissions (FD-II control). A comparison of these three control methods is shown in Fig. 13 (a)–(m), and the results showed the following:

(1) The system fuel consumption with FD control was 0%–20% lower than that with ZD control under all working conditions, if emissions were not considered. Even if emissions were limited, the fuel efficiency of the tractor was still better than that with ZD control; however, under some heavy load operations, the system fuel consumption of the FD control was slightly higher than that of ZD control by 0%–5%.
(2) ZD control was equivalent to treating the CVT as a mechanical shift transmission with four gears, making the CVT tractor theoretically save 0%–20% more fuel than a mechanical shift-driven tractor.
(3) If the emissions were not limited, using FD control resulted in significantly higher smoke levels under a partially heavy load and medium load, in contrast to the zero-emission control. However, if emissions were limited, this situation significantly improved and the fuel economy of the CVT tractor was not affected.

5. Conclusion

In this study, we analyzed the fuel economy of a hydrostatic power-split tractor CVT and reached the following conclusions:

(1) The CVT, based on the Simpson planetary gear set, consumes more energy on the low-speed side of the range due to parasitic power, so the high-speed side of the range should be used preferentially to reduce energy consumption. The low range should be selected when the CVT is operating near the shift point. The CVT has the lowest energy consumption when the pump displacement is reduced to zero.
(2) Reducing the coefficient of viscous damping f_p on the pump shaft can reduce energy consumption, as can reducing the coefficient of viscous damping f_m on the motor shaft. A fixed bent-axis motor is recommended to reduce energy loss from friction. The speed of the engine should be lowered as long as its output power can meet the requirements of operation of the tractor.
(3) Increasing the transmission ratio of the gear pair between the input shaft and the pump shaft can significantly reduce energy consumption. This is the only mechanical parameter that has a significant impact on the energy consumption of the CVT while keeping the speed regulating range of CVT unchanged. It is essential to ensure that the working pressure of the pump and motor does not exceed the manufacturer's recommended maximum value.
(4) Improving fuel economy of tractors can be achieved by optimizing design parameters and power matching strategies. For the hydrostatic power-split CVT studied, increasing the transmission ratio of the gear pair between the input and pump shaft can reduce system fuel consumption by 2%–14%. After parameter optimization, full-displacement control can further reduce fuel

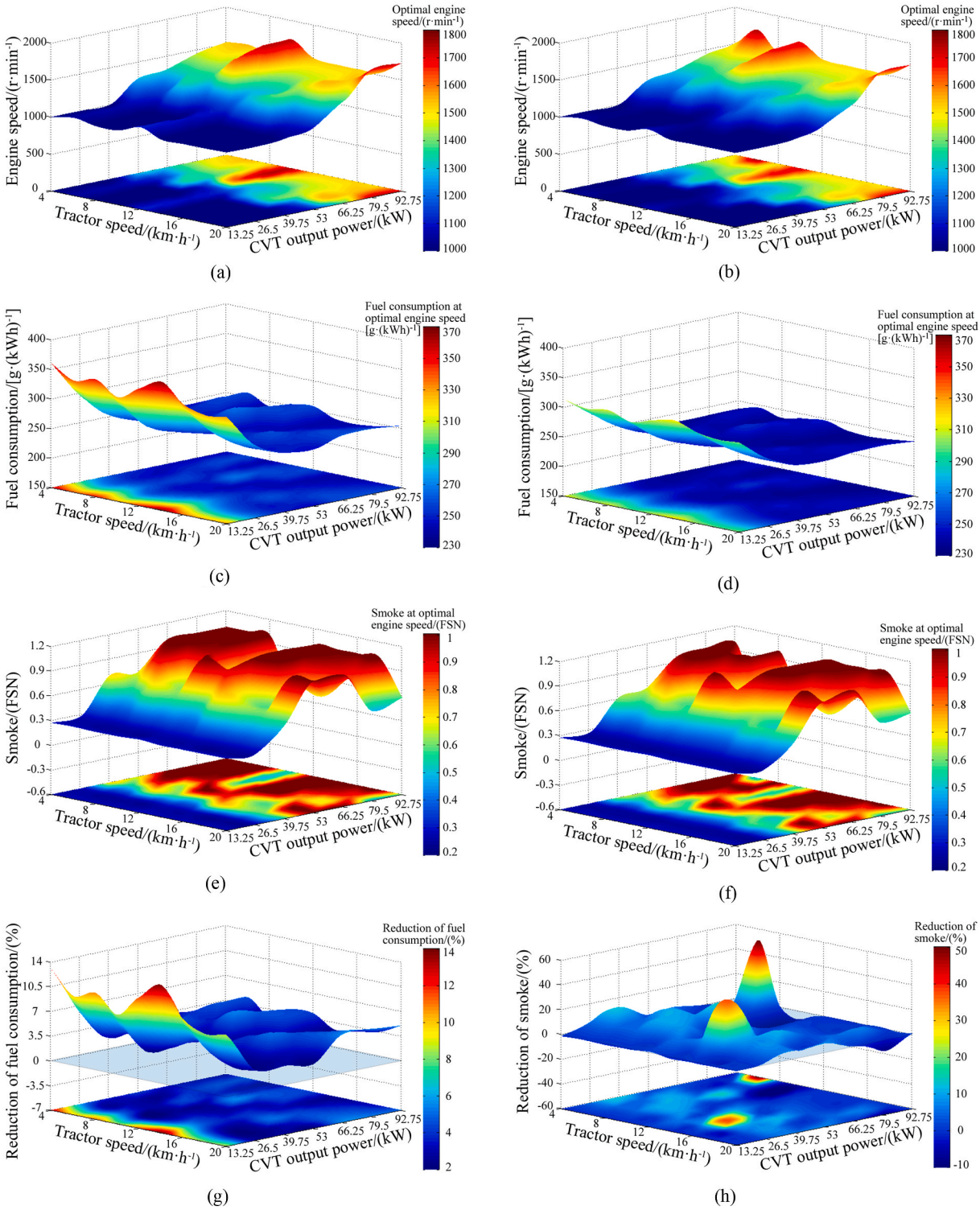

Fig. 12. Results of the matching-based fuel economy of the "engine-transmission" system before and after the optimization of transmission ratio i_3. (a) Optimum engine speed when $i_3 = 0.678$. (b) Optimum engine speed when $i_3 = 1$. (c) System fuel consumption corresponding to the optimum engine speed when $i_3 = 0.678$. (d) System fuel consumption corresponding to the optimum engine speed when $i_3 = 1$. (e) Level of smoke corresponding to the optimum engine speed when $i_3 = 0.678$. (f) Level of smoke corresponding to the optimum engine speed when $i_3 = 1$. (g) Effects on system fuel consumption after changing i_3 from 0.678 to 1; (h) Effect on the level of smoke after changing i_3 from 0.678 to 1.

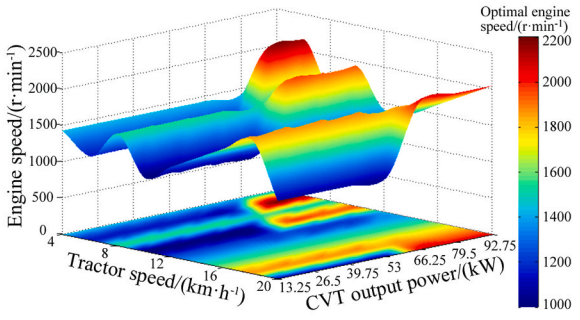
Optimal engine speed/(r·min-1)
Engine speed/(r·min-1)
Tractor speed/(km·h-1)
CVT output power/(kW)

(a)

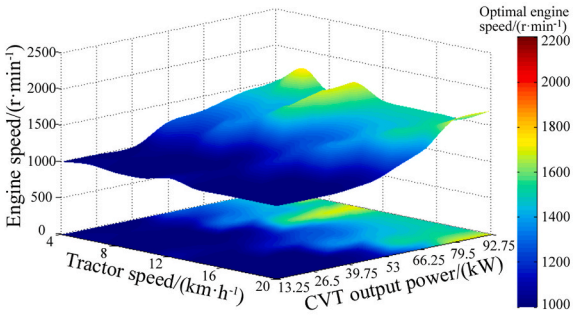
Optimal engine speed/(r·min-1)
Engine speed/(r·min-1)
Tractor speed/(km·h-1)
CVT output power/(kW)

(b)

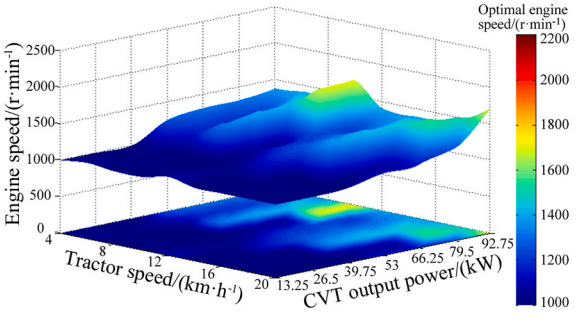
Optimal engine speed/(r·min-1)
Engine speed/(r·min-1)
Tractor speed/(km·h-1)
CVT output power/(kW)

(c)

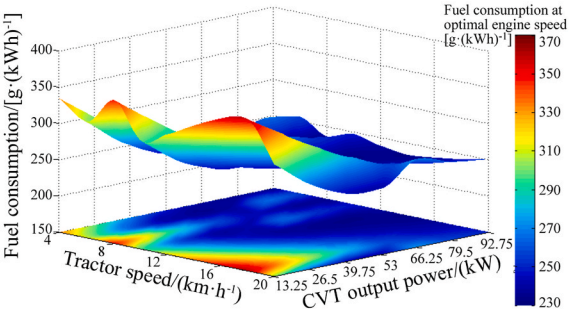
Fuel consumption at optimal engine speed [g·(kWh)-1]
Fuel consumption/[g·(kWh)-1]
Tractor speed/(km·h-1)
CVT output power/(kW)

(d)

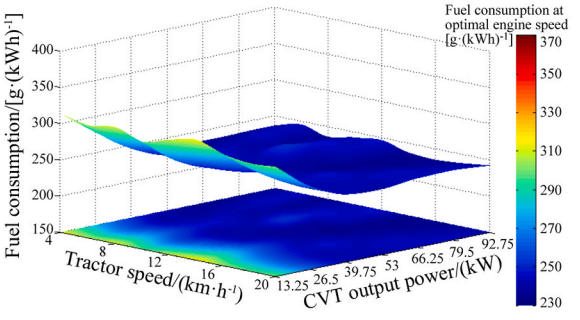
Fuel consumption at optimal engine speed [g·(kWh)-1]
Fuel consumption/[g·(kWh)-1]
Tractor speed/(km·h-1)
CVT output power/(kW)

(e)

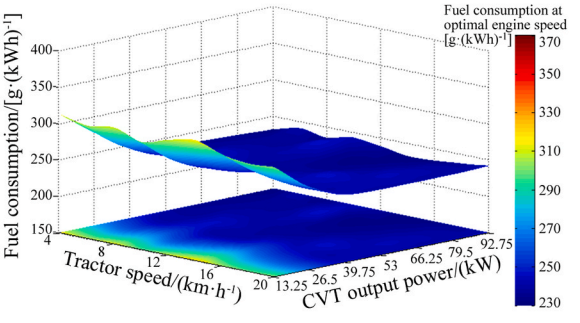
Fuel consumption at optimal engine speed [g·(kWh)-1]
Fuel consumption/[g·(kWh)-1]
Tractor speed/(km·h-1)
CVT output power/(kW)

(f)

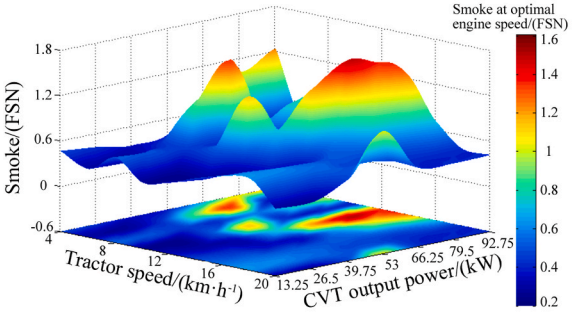
Smoke at optimal engine speed/(FSN)
Smoke/(FSN)
Tractor speed/(km·h-1)
CVT output power/(kW)

(g)

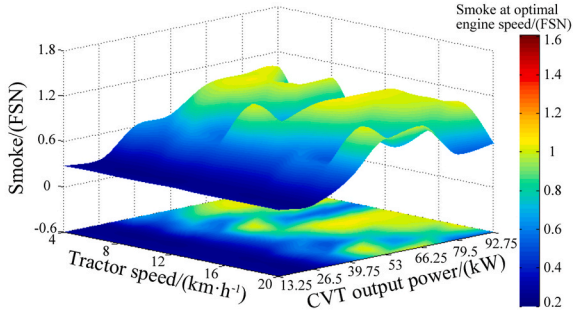
Smoke at optimal engine speed/(FSN)
Smoke/(FSN)
Tractor speed/(km·h-1)
CVT output power/(kW)

(h)

Fig. 13. Matching-based fuel economy results of the "engine-transmission" system before and after optimization of the control strategy. (a) Optimal engine speed under ZD control. (b) Optimal engine speed under FD-I control. (c) Optimal engine speed under FD-II control. (d) System fuel consumption based on ZD control. (e) System fuel consumption based on FD-I control. (f) System fuel consumption based on FD-II control. (g) Level of smoke based on ZD control. (h) Level of smoke based on FD-I control. (i) Level of smoke based on FD-II control. (j) Effects on system fuel consumption when ZD control is replaced with FD-I control. (k) Effects on system fuel consumption when ZD control is replaced with FD-II control. (l) Effects on the level of smoke when ZD control is replaced with FD-I control. (m) Effects on the level of smoke when ZD control is replaced with FD-II control.

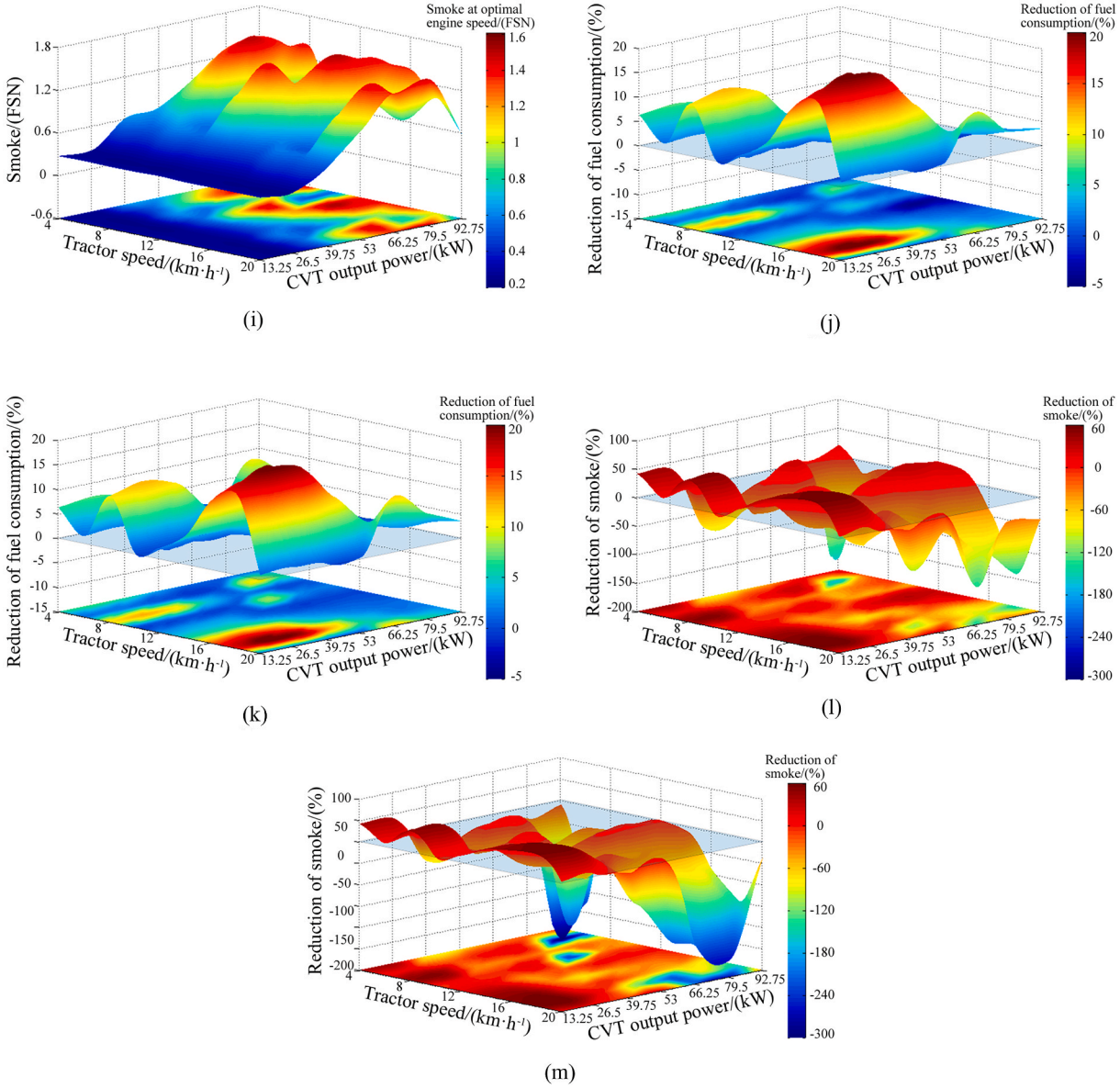

Fig. 13. (*continued*).

consumption by 0%–20% compared to ZD control. Engine emission limits via CVT control strategies do not significantly affect fuel economy.

These conclusions apply to input-coupled hydrostatic power-split transmissions using standard planetary gears, widely used in CVT tractors. Future research will consider fuel economy in other types of tractor CVTs.

Author contribution statement

Guangming Wang: conceived and designed the experiments; performed the experiments; analyzed and interpreted the data; wrote the paper.

Yehui Zhao: analyzed and interpreted the data; wrote the paper.

Yue Song: contributed reagents, materials, analysis tools or data; wrote the paper.

Lijun Xue: analyzed and interpreted the data; wrote the paper.

Xiaohan Chen: analyzed and interpreted the data; wrote the paper.

Funding statement

This work was supported by the Shandong Provincial Natural Science Foundation [grant number ZR2020QE163] and the Shandong Provincial Key Research and Development Program [grant number 2018GNC112008].

Date availability statement

Data will be made available on request.

Declaration of competing interest

The authors declare the following financial interests/personal relationships which may be considered as potential competing interests:

Guangming Wang reports financial support was provided by Shandong Provincial Natural Science Foundation.

References

[1] A.K. Agarwal, Prashumn, K. Chandra, Di-ethyl ether-diesel blends fuelled off-road tractor engine: Part-I: technical feasibility, Fuel 308 (2022), 121972.
[2] K. Velmurugan, J. Arunprasad, R. Thirugnanasambantham, Agricultural tractor engine combustion in dual-fuel mode: optimization of pilot fuel injection, Mater. Today: Proc. 33 (2020) 3271–3276.
[3] V. Venkatesan, N. Nallusamy, P. Nagapandiselvi, Performance and emission analysis on the effect of exhaust gas recirculation in a tractor diesel engine using pine oil and soapnut oil methyl ester, Fuel 290 (2021), 120077.
[4] A. Janulevičius, A. Čiplienė, Estimation of engine CO_2 and NO_x emissions and their correlation with the not-to-exceed zone for a tractor ploughing fields of various sizes, J. Clean. Prod. 198 (2018) 1583–1592.
[5] G. Wang, Y. Song, J. Wang, M. Xiao, Y. Cao, W. Chen, J. Wang, Shift quality of tractors fitted with hydrostatic power split CVT during starting, Biosyst. Eng. 196 (2020) 183–201.
[6] K.T. Renius, R. Resch, Continuously variable tractor transmissions, in: 2005 Agricultural Equipment Technology Conference, ASAE, 2005, pp. 1–37.
[7] A.Y. Bukashkin, R.Y. Dobretsov, Y.V. Galyshev, Split transmission of tractor with automatic gearbox, Procedia Eng. 206 (2017) 1728–1734.
[8] L. Xue, H. Jiang, Y. Zhao, J. Wang, G. Wang, M. Xiao, Fault diagnosis of wet clutch control system of tractor hydrostatic power split continuously variable transmission, Comput. Electron. Agric. 194 (2022), 106778.
[9] K.T. Renius, Fundamentals of Tractor Design, Springer Nature Switzerland AG, 2020.
[10] P. Linares, V. Méndez, H. Catalán, Design parameters for continuously variable power-split transmissions using planetaries with 3 active shafts, J. Terramechanics 47 (5) (2010) 323–335.
[11] U. Blumenthal, T. Hansen, R.O. Hartmann, Claas CVT development for different applications in commercial vehicles, in: International Off-Highway & Powerplant Congress & Exposition, SAE, 2000, pp. 2000–2001, 2642.
[12] M. Cammalleri, D. Rotella, Functional design of power-split CVTs: an uncoupled hierarchical optimized model, Mech. Mach. Theor. 116 (2017) 294–309.
[13] F. Liu, W. Wu, J. Hu, S. Yuan, Design of multi-range hydro-mechanical transmission using modular method, Mech. Syst. Signal Process. 126 (2019) 1–20.
[14] W. Chen, Z. Xu, Y. Wu, Y. Zhao, G. Wang, M. Xiao, Analysis of the shift quality of a hydrostatic power split continuously variable cotton picker, Mech. Sci. 12 (1) (2021) 589–601.
[15] A. Rossetti, A. Macor, Multi-objective optimization of hydro-mechanical power split transmissions, Mech. Mach. Theor. 62 (2013) 112–128.
[16] A. Rossetti, A. Macor, M. Scamperle, Optimization of components and layouts of hydromechanical transmissions, Int. J. Fluid Power 18 (2) (2017) 123–134.
[17] Y. Xia, D. Sun, D. Qin, X. Zhou, Optimisation of the power-cycle hydro-mechanical parameters in a continuously variable transmission designed for agricultural tractors, Biosyst. Eng. 193 (2020) 12–24.
[18] E. İnce, M.A. Güler, On the advantages of the new power-split infinitely variable transmission over conventional mechanical transmissions based on fuel consumption analysis, J. Clean. Prod. 244 (2020), 118795.
[19] A. Rossetti, A. Macor, Control strategies for a powertrain with hydromechanical transmission, Energy Proc. 148 (2018) 978–985.
[20] A. Rossetti, A. Macor, A. Benato, Impact of control strategies on the emissions in a city bus equipped with power-split transmission, Transport. Res. Transport Environ. 50 (2017) 357–371.
[21] A. Wang, J. Xu, M. Zhang, Z. Zhai, G. Song, M. Hatzopoulou, Emissions and fuel consumption of a hybrid electric vehicle in real-world metropolitan traffic conditions, Appl. Energy 306 (2022), 118077.
[22] Y. Xing, C. Lv, D. Cao, C. Lu, Energy oriented driving behavior analysis and personalized prediction of vehicle states with joint time series modeling, Appl. Energy 261 (2020), 114471.
[23] Q. Zhou, J. Li, B. Shuai, H. Williams, Y. He, Z. Li, H. Xu, F. Yan, Multi-step reinforcement learning for model-free predictive energy management of an electrified off-highway vehicle, Appl. Energy 255 (2019), 113755.
[24] G. Wang, Study on Characteristics, Control and Fault Diagnosis of Tractor Hydro-Mechanical CVT, Nanjing Agricultural University, Nanjing, 2014 (Ph.D. thesis).
[25] R. Resch, Leistungsverzweigte Mehrbereichsfahrantriebe mit Kettenwandler, TU München, München, 2004 (Ph.D. thesis).
[26] J. Seeger, Wirkungsgraduntersuchung des systems “Dieselmotor-Leistungsverzweigtes Getriebe, Olhydraulik Pneum. 45 (2001) 672–677.
[27] M. Zhang, J. Wang, J. Wang, Z. Guo, F. Guo, Z. Xi, J. Xu, Speed changing control strategy for improving tractor fuel economy, Trans. Chin. Soc. Agric. Eng. 36 (1) (2020) 82–89.
[28] K.T. Renius, Untersuchungen zur Reibung zwischen Kolben und Zylinder bei Schragscheiben-Axialkolbenmaschinen, TU Braunschweig, Braunschweig, 1973 (Ph.D. thesis).